Spatial dynamics of species with annually synchronized emergence of adults*

Zhenguo Bai[a], Yijun Lou[†b], and Xiao-Qiang Zhao[c]

[a] School of Mathematics and Statistics, Xidian University, Xi'an, 710126, China
[b] Department of Applied Mathematics, Hong Kong Polytechnic University, Hong Kong SAR, China
[c] Department of Mathematics and Statistics, Memorial University of Newfoundland, St. John's, NL A1C 5S7, Canada

Abstract. Synchronized maturation has been extensively studied in biological science on its evolutionary advantages. This paper is devoted to the study of the spatial dynamics of species growth with annually synchronous emergence of adults by formulating an impulsive reaction-diffusion model. With the aid of the discrete-time semiflow generated by the one-year solution map, we establish the existence of the spreading speed and traveling waves for the model on an unbounded spatial domain. It turns out that the spreading speed coincides with the minimal speed of traveling waves, regardless of the monotonicity of the birth rate function. We also investigate the model on a bounded domain with a lethal exterior to determine the critical domain size to reserve species persistence. Numerical simulations are illustrated to confirm the analytical results and to explore the effects of the emergence maturation delay on the spatial dynamics of the population distribution. In particular, the relationship between the spreading speed and the emergence maturation delay is found to be counterintuitively variable.

Key words: Impulsive reaction-diffusion model, maturation delay, traveling waves, spreading speed, critical domain size

AMS Subject Classification: 35K57, 37N25, 92D25

---

*This research was supported in part by the NSF of China [11971369, 12071393], the Fundamental Research Funds for the Central Universities [JB210711], the General Research Fund from The Hong Kong Research Grants Council [15304821], and the NSERC of Canada [RGPIN-2019-05648].

[†] Corresponding author: yijun.lou@polyu.edu.hk

1 Introduction

Reproductive synchrony refers to the temporal clustering of reproductive events (mating, spawning, and/or births) among individuals within a restricted time window, which is widely documented in plant and animal populations [21, 23]. It may arise simply as an adaptive mechanism of environmental seasonality in climate or resources. It may also increase individual offspring survival by reducing the per capita predation rate or promoting communal breeding for some species [23]. Reproductive synchrony may happen in seasonally, lunar or every-other-day cycles. Breaking the spawning synchrony is regarded to be a threat to coral persistence [25]. Interesting modeling studies have been performed to understand the mechanisms of reproductive synchrony and its effect on population growth. To catch the every-other-day egg laying synchrony pattern observed in colonies of gulls, juvenile-adult structured difference equation models were proposed and analyzed in [28, 29]. By stratifying the adult individuals into two classes: reproductively active and inactive adults, the existence of a synchronous 2-cycle composite of fixed points can indicate the synchronized reproduction. Another well-accepted modeling approach to include the reproductive synchrony is by dividing the cycle into two seasons, a non-reproduction season and a short reproduction season. By taking the extreme value of a short reproduction season, impulsive differential systems can be formulated [14, 30, 32]. If the duration of the cycle is fixed, for example one year, then the differential system with impulsive reproduction rate may define an abstract difference equation or a discrete-time semiflow which describes the evolution from this year's density of offspring to that of the next year [11, 32]. Following this idea, the persistence and critical domain size for populations with two sexes and a short reproductive season was investigated in [11]. A reaction-diffusion equation model with impulsive seasonal reproduction and individual dispersal [6] was proposed and the critical domain results were established. An impulsive integro-differential model was formulated and analyzed to capture the dynamics of an invading species with an impulsive reproduction stage and a nonlocal dispersal stage in [32]. Considering the potential habitat shift driven by climate change, the persistence or extinction problem of moving animal species with birth pulse was investigated in [30]. All these studies and references therein greatly improve understanding on reproductive synchrony and proposes interesting mathematical questions.

Following the coordinated reproduction, synchronized emergence of matured individuals has also been reported through observational studies for some species, and synchronous hatching and emergence occurs in many taxa in egg-laying animals [24]. For example, synchronized maturation in natural populations of *Xiphophorus variatus* is reported [3] and synchronized emergence of adult cicadas is widely observed in 13- and 17-year cycles [9]. Although there have been extensive biological observations and experiments on the possible advantages underlying the synchronized maturation phenomenon, including reduced mortality due to avain predation, fungal infection, environmental factors, and senescence [31], few modeling studies have been performed to qualitatively and quantitatively evaluate the impact of synchronous development activity on population persistence and invasion in a spatially explicit habitat.

Our purpose is to formulate a spatial population growth model with synchronized emergence of matured individuals by adopting the impulsive reaction-diffusion modeling idea for coordinated reproduction and impulsive pesticide applications in dispersing population growth (see aforementioned references and [7, 12, 16, 19]). To do that, the whole species is divided into two growth stages, immature and adult stage, which enables us to distinguish the heterogeneity of individuals in different stages on the reproductive potential, ability to disperse and mortality rates. Then the impulse term can be derived to describe the maturation pulse perturbation at fixed timing of one cycle. In particular, the following biological characteristics will be assumed:

- (B1) The species can be divided into two development stages for immature and matured individuals, respectively. Within each stage, all individuals share the same demographic parameters, such as the birth, death and dispersal rates.
- (B2) Matured individuals reproduce offsprings at the beginning of year, and they reach maturation at certain time $\tau \in (0, 1)$ in the same year. That is, newborns mature at time τ in each year, and hence, there is synchronized emergence of matured individuals at time τ of each year.
- (B3) There is no density-dependent regulation on the immatures during development. Both immature and matured individuals may disperse within a habitat, at possibly different diffusion rates.

The organization of this paper is as follows. In section 2, including the above characteristics in a population growth model, we formulate an age-structured reaction-diffusion model with an impulsive term to describe the synchronized emergence of matured individuals. A discrete-time semiflow can be further abstracted from this model. In section 3, we investigate the property of such a discrete-time semiflow and establish the existence of spreading speeds and traveling waves, which shed light on the spatial patterns and invading rates of species. In section 4, we study the critical domain size determining the successful establishment of the population, persistence or extinction. At last, we present numerical simulations to evaluate the impact of synchronized maturation emergence on spatial population dynamics and discuss possible extensions through relaxing modeling assumptions of the current research.

Figure 1: The diagram describes the evolution of population dynamics for the adult stage $u_n(t,x)$ and juvenile stage $v_n(t,x)$ at time $n+t$ and space location x, here $t \in [0,1]$ and n represents the n-th year. The adult population density at location x and at the beginning and end of the n-th year can be represented as $N_n(x) = u_n(0,x)$ and $N_{n+1}(x) = u_n(1,x)$, respectively. Note that there is an impulsive recruitment rate $\mathcal{R}(x; N_n)$ to the adult stage at the time instant $n+\tau$ in the n-th year.

2 Model formulation

To describe the population growth with annually synchronized maturation driven by coordinated offspring reproduction, without loss of generality, we assume that adults reproduce at the beginning of the n-th year, with $n \in \mathbb{N} = \{0, 1, 2, \cdots\}$. Let $u_n(t, x)$ be the adult population density at time $t \in [0, 1]$ and $x \in \mathbb{R}$ within year $n \in \mathbb{N}$. Then the adult population densities $N_n(x)$ and $N_{n+1}(x)$ at the beginning of year n and year $n+1$ follow the following balance laws

$$N_n(x) = u_n(0, x) \text{ and } N_{n+1}(x) = u_n(1, x).$$

The demographic process is illustrated in Fig. 1.

At the beginning of n-th year and spatial location x, the immature individuals are reproduced at density $g(N_n(x))$, dependent on the adult population density. These immature individuals develop into the adult stage after time τ, the synchronized maturation duration. Due to the synchronized maturation in the n-th year, the adult population density $u_n(t, x)$ has an abrupt increase at time $t = \tau$ and location x, which can be characterized by an impulsive force at that moment

$$u_n(t^+, x) = u_n(t, x) + \mathcal{R}(x; N_n) \text{ when } t = \tau, \tag{2.1}$$

where $u_n(t, x) = u_n(t^-, x)$ and $\mathcal{R}(x; N_n)$ describes the density of newly emerging matured individuals. During the period of their development, immature individuals can perform random diffusion with diffusion rate $D_I > 0$ and are subject to a natural death rate $d_I > 0$. Let $v_n(t, x)$ be the immature population density at time $t \in [0, 1]$ and $x \in \mathbb{R}$. Then $v_n(0, x) = g(N_n(x))$ and its evolution dynamics is governed by $\dfrac{\partial v_n}{\partial t} = D_I \dfrac{\partial^2 v_n}{\partial x^2} - d_I v_n$. Let T_t be the time-t map of the linear equation $\frac{\partial v}{\partial t} = D_I \frac{\partial^2 v}{\partial x^2} - d_I v$. It follows that the density of newly emerging matured individuals at location x and time $n + \tau$ of the n-th year can be expressed as

$$\mathcal{R}(x; N_n) = \Big(T_\tau g(N_n(\cdot))\Big)(x) = \underbrace{e^{-d_I \tau}}_{\substack{\text{survival probability} \\ \text{through maturation}}} \int_{\mathbb{R}} \underbrace{\Gamma(D_I \tau, x - y)}_{\substack{\text{diffusion to location } x \\ \text{during maturation}}} \underbrace{g(N_n(y))}_{\substack{\text{born at} \\ \text{location } y}} dy, \tag{2.2}$$

where $\Gamma(t, x) = \frac{1}{\sqrt{4\pi t}} e^{-\frac{x^2}{4t}}$ is the fundamental solution associated with the partial differential operator $\partial_t - \frac{\partial^2}{\partial x^2}$. The above term accounts the immatures surviving through the maturation period with an exponential surviving probability and moving from location y to location x in a normally distributed way.

At other time instances of one year, the adult population density can be described by a reaction-diffusion equation

$$\frac{\partial u_n}{\partial t} = D_M \frac{\partial^2 u_n}{\partial x^2} + f(u_n) \text{ when } 0 < t \le 1,\ t \ne \tau, \tag{2.3}$$

where $D_M > 0$ is the rate of adult random diffusion and $f(\cdot)$ is the death rate function, including both density-independent and density-dependent mortalities.

Since the newly matured individuals can be expressed by a term of adult population density, the above arguments summarize the following system to describe the spatial evolution of adult population density with an annual impulsive maturation emergence

$$\begin{cases} \dfrac{\partial u_n}{\partial t} = D_M \dfrac{\partial^2 u_n}{\partial x^2} + f(u_n), & 0 < t \leq 1,\ t \neq \tau,\ x \in \mathbb{R}, \\ u_n(t^+, x) = u_n(t, x) + \mathcal{R}(x; N_n), & t = \tau, \\ u_n(0, x) = N_n(x), & n = 0, 1, 2, \ldots \\ N_{n+1}(x) = u_n(1, x). \end{cases} \tag{2.4}$$

Here the initial data is $u_0(0, x) = N_0(x)$, $\forall x \in \mathbb{R}$. Various types of functions have been extensively used to approximate the birth and death rates in population growth models [6, 14, 16, 32]. For example, the Beverton-Holt function $g_1(N) = \frac{pN}{q+N}$ with positive constants p and q, and the Ricker function $g_2(N) = Ne^{r-kN}$ with positive constants r and k are typical ones for the birth rate function, while $f_1(N) = -aN - bN^2$ with positive constants a and b is widely used to describe the joint effect of natural and density-dependent death rates. Motivated by these functional responses, we assume that the death rate function f and birth function g satisfy the following assumptions throughout this paper:

(H1) f is a locally Lipschitz continuous function in $\mathbb{R}_+$, $f(0) = 0 > f'(0)$ and $f(N)/N$ is strictly decreasing in N.

(H2) g is a locally Lipschitz continuous function in $\mathbb{R}_+$, $g(0) = 0 < g'(0)$ and $g(N) > 0$ for $N > 0$. Moreover, $g(N)/N$ is nonincreasing for N, and there exists $\bar{N} > 0$ such that $g(\bar{N}) \leq \bar{N}$.

(H3) There are real numbers $F > 0$, $G > 0$, $\sigma_f > 0$, $\sigma_g > 0$, $\nu_f > 1$ and $\nu_g > 1$ such that $f(N) \geq f'(0)N - FN^{\nu_f}$ for $0 \leq N \leq \sigma_f$ and $g(N) \geq g'(0)N - GN^{\nu_g}$ for $0 \leq N \leq \sigma_g$.

It is easy to see that if both $f''(0)$ and $g''(0)$ exist, then (H3) holds true with $\nu_f = \nu_g = 2$. Clearly, the aforementioned functions f_1, g_1 and g_2 satisfy the above assumptions. However, we should point out that two birth functions share different monotonicity properties: $g_1(N)$ is strictly increasing, while $g_2(N)$ is not. Different analytical techniques will be employed to investigate the spatial dynamics for two scenarios (see subsections in Sections 3 and 4).

Although the model (2.4) admits a maturation impulse, it is interesting to observe that the impulse occurs at instants τ of the n-th year, that is, this abrupt change happens periodically. This motivates us to consider the one-year time map of system (2.4). Let M_t be the solution map of $\frac{\partial u}{\partial t} = D_M \frac{\partial^2 u}{\partial x^2} + f(u)$. For a distribution of adult density $\phi(x)$ at location

x at the beginning of the year, the distribution at time τ is $M_\tau(\phi)(x)$ due to individual movement and death, and at time τ^+, it becomes $[M_\tau(\phi)+T_\tau g(\phi)](x)$ because of coordinated maturing adults. After that, the spatial distribution follows (2.3) in the remaining $[\tau,1]$ interval and the distribution at the end of year becomes $M_{1-\tau}[M_\tau(\phi)+T_\tau g(\phi)](x)$. Thus, the time-one solution map of system (2.4) is

$$Q[\phi](x) = M_{1-\tau}[M_\tau(\phi)+T_\tau g(\phi)](x), \quad x\in\mathbb{R}. \tag{2.5}$$

For any time instant $\tilde{t}\geq 0$, there is a unique decomposition $\tilde{t} = \lfloor\tilde{t}\rfloor + t$, where $t\in[0,1)$ and $\lfloor\tilde{t}\rfloor$ denotes the nearest integer less than or equal to $\tilde{t}$. It then follows that the time-$\tilde{t}$ solution map of system (2.4) can be expressed as

$$\Phi_{\tilde{t}}[\phi](x) = \begin{cases} M_{\tilde{t}-\lfloor\tilde{t}\rfloor}\circ Q^{\lfloor\tilde{t}\rfloor}[\phi](x), & 0\leq\tilde{t}-\lfloor\tilde{t}\rfloor\leq\tau, \\ M_{\tilde{t}-\lfloor\tilde{t}\rfloor-\tau}\circ[M_\tau(Q^{\lfloor\tilde{t}\rfloor}[\phi])+T_\tau g(Q^{\lfloor\tilde{t}\rfloor}[\phi])](x), & \tau<\tilde{t}-\lfloor\tilde{t}\rfloor<1 \end{cases}$$

for any given initial value $\phi = N_0$. Further, a straightforward verification shows that $\Phi_{\tilde{t}}\circ\Phi_1 = \Phi_{\tilde{t}+1}$ for all $\tilde{t}\geq 0$. Note that $\Phi_{\tilde{t}}[\phi]$ is continuous in $\tilde{t}\in\mathbb{R}_+\setminus\{n+\tau:\ n=0,1,2,\ldots\}$ for any given ϕ, and $\Phi_{\tilde{t}}[\phi]$ is continuous in ϕ uniformly for $\tilde{t}$ in any bounded interval. Thus, $\{\Phi_{\tilde{t}}\}_{\tilde{t}\geq 0}$ can be regarded as a 1-periodic semiflow in a weak sense (i.e., the traditional joint continuity in $(\tilde{t},\phi)$ is replaced by the aforementioned two continuities). Since the Poincaré map of $\{\Phi_{\tilde{t}}\}_{\tilde{t}\geq 0}$ is exactly $\Phi_1 = Q$, the evolution dynamics of system (2.4) can be investigated via the following discrete-time recursion

$$N_{n+1}(x) = Q[N_n](x), \quad x\in\mathbb{R},\ n\geq 0. \tag{2.6}$$

For this reduction, we refer to [36, Section 3.1], [17, Section 2] and [32, 33]. In the rest of this paper, we will focus on the evolution dynamics of the discrete-time semiflow $\{Q^n\}_{n\geq 0}$ associated with system (2.6) in the cases of unbounded and bounded spatial domains.

3 Spreading speeds and traveling waves

In this section, we study the spreading speed and traveling waves of system (2.6) with two different kinds of birth functions. For notational simplicity, we drop subscript n for $u_n(t,x)$ in (2.4) and rewrite it as $u(t,x)$ for $t\in[0,1]$.

3.1 Scenario 1: The birth function g is monotone

We first investigate the global dynamics of the spatially homogeneous version of (2.4):

$$\begin{cases} \dfrac{du}{dt} = f(u), & 0 < t \leq 1,\ t \neq \tau, \\ u(t^+) = u(t) + e^{-d_I \tau} g(N_n), & t = \tau, \\ u(0) = N_n, & n = 0, 1, 2, \ldots \\ N_{n+1} = u(1). \end{cases} \tag{3.1}$$

Similar to the formulation of the discrete-time recursion (2.6), this impulsive ordinary differential model gives rise to a discrete-time dynamical system:

$$N_{n+1} = \hat{S}(N_n) := S_{1-\tau}(S_\tau(N_n) + e^{-d_I \tau} g(N_n)), \quad n \geq 0, \tag{3.2}$$

where S_t is the time-t map of system $\frac{du}{dt} = f(u)$ with $t \in [0, 1]$. Then it is easy to show that $\hat{S}$ is monotone and strongly subhomogeneous based on the assumptions on growth functions (H1)-(H3) (see [36]). For the recursion derived from the impulsive ordinary differential system $\hat{S}$, we can explicitly compute that

$$\hat{S}'(0) := e^{f'(0)} + g'(0) e^{f'(0)(1-\tau) - d_I \tau}$$

via the linearized system of (3.1) at zero. In view of (H2), it follows that for any $\hat{N} \geq \overline{M} := (1 + e^{-d_I \tau})\bar{N}$, $[0, \hat{N}]$ is positively invariant for system (3.2) in the sense that if $0 \leq N_0 \leq \hat{N}$, then $0 \leq N_n \leq \hat{N}$ for all $n \geq 1$. Therefore, $\hat{S}$ is a continuous and compact map on $\mathbb{R}$. The following result is a straightforward consequence of [36, Lemma 2.2.1 and Theorem 2.3.4].

Lemma 3.1. *The following statements are valid:*

(i) If $\hat{S}'(0) \leq 1$, then $N_n = 0$ is globally asymptotically stable for (3.2) in $\mathbb{R}_+$.

(ii) If $\hat{S}'(0) > 1$, then (3.2) admits a unique fixed point $\beta > 0$ which is globally asymptotically stable in $\mathbb{R}_+ \setminus \{0\}$.

To study the propagation dynamics of (2.6), we assume that $\hat{S}'(0) > 1$ in the rest of this subsection to guarantee that the operator $\hat{S}$ admits a positive fixed point β which is globally asymptotically stable. Let $\mathcal{C}$ be the set of all bounded and continuous functions from $\mathbb{R}$ to $\mathbb{R}$. For any ϕ, $\psi \in \mathcal{C}$, we write $\phi \geq \psi$ if $\phi(x) \geq \psi(x)$ for all $x \in \mathbb{R}$; and $\phi > \psi$ if $\phi \geq \psi$ but $\phi \neq \psi$. Define

$$\|\phi\|_{\mathcal{C}} = \Sigma_{k=1}^{\infty} \frac{\max_{|x| \leq k} |\phi(x)|}{2^k}, \qquad \forall \phi \in \mathcal{C},$$

Then $(\mathcal{C}, \|\cdot\|_{\mathcal{C}})$ is a normed space. It is easy to see that the norm $\|\cdot\|_{\mathcal{C}}$ induces the standard compact open topology on $\mathcal{C}$, that is, a sequence of points ϕ^n converges to ϕ in $\mathcal{C}$ if the sequence $\phi^n(x)$ of functions converges to $\phi(x)$ uniformly for x in any compact subset of $\mathbb{R}$.

For a given number $r > 0$, define $\mathcal{C}_r := \{\phi \in \mathcal{C} : 0 \le \phi(x) \le r, \ \forall x \in \mathbb{R}\}$. Thus, we are able to use the theory developed in [18] to establish the propagation dynamics for system (2.6).

Theorem 3.1. *If $\hat{S}'(0) = e^{f'(0)} + g'(0)e^{f'(0)(1-\tau)-d_I\tau} > 1$, then system* (2.6) *admits a spreading speed c^* in the sense that*

(i) For any $c > c^*$, if $\phi \in \mathcal{C}_\beta$ with $0 \le \phi \ll \beta$ and $\phi(x) = 0$ outside a bounded interval, then $\lim_{n\to\infty, |x|\ge cn} Q^n[\phi](x) = 0$.

(ii) For any $c < c^*$, if $\phi \in \mathcal{C}_\beta \setminus \{0\}$, then $\lim_{n\to\infty, |x|\le cn} Q^n[\phi](x) = \beta$.

Proof. For any $\phi \in \mathcal{C}$, let $R[\phi](x) := \phi(-x)$ be the reflection operator and $\overline{T}_y[\phi](x) := \phi(x-y)$ be the translation operator for a given $y \in \mathbb{R}$. Based on the definition of the time-one map Q in (2.5), we show that the following statements are valid for Q:

(A1) $Q[R[\phi]] = R[Q[\phi]]$, $\overline{T}_y[Q[\phi]] = Q[\overline{T}_y[\phi]]$, $\forall y \in \mathbb{R}$.

(A2) $Q : \mathcal{C}_\beta \to \mathcal{C}_\beta$ is continuous with respect to the compact open topology.

(A3) $Q[\mathcal{C}_\beta]$ is precompact in $\mathcal{C}_\beta$.

(A4) Q is order preserving in the sense that $Q[\phi] \ge Q[\psi]$ whenever $\phi \ge \psi$.

(A5) $Q : [0,\beta] \to [0,\beta]$ admits two fixed points 0 and β, and for any $\phi \in \mathcal{C}_\beta$ with $0 < \phi \le \beta$, there holds $\lim_{n\to\infty} Q^n[\phi] = \beta$.

If $u(\tilde{t}, x)$ is a solution to (2.4) with $n = \lfloor \tilde{t} \rfloor$ and $t = \tilde{t} - \lfloor \tilde{t} \rfloor \in [0,1)$, then $u(\tilde{t}, x+y)$, $\forall y \in \mathbb{R}$ and $u(\tilde{t}, -x)$, are also solutions. Therefore, (A1) holds for the map Q. The property (A2) can be established by the arguments similar to those in [34, Lemma 2.2]. Note that $M_{1-\tau}$ is compact with respect to the compact open topology (see, e.g., the proof of Lemma 3.3). Thus, Q is compact on $\mathcal{C}_\beta$, and hence (A3) holds. Further, since the birth function g is monotonically increasing, Q is order preserving and (A4) holds. By statement (ii) in Lemma 3.1, we see that condition (A5) is valid for Q. Further, we can verify that Q is subhomogeneous on $\mathcal{C}_\beta$ in the sense that $Q[\alpha\phi] \ge \alpha Q[\phi]$ for any $\phi \in \mathcal{C}_\beta \setminus \{0\}$ and $\alpha \in (0,1)$. Therefore, [18, Theorem 2.11, 2.15 and Corollary 2.16] and [17, Theorem A] imply that (2.6) admits a spreading speed c^* satisfying (i) and (ii). □

Next we use the linear operators approach (see, e.g., [22]) to estimate c^*. For any $\epsilon \in (0,1)$, let L_t^ϵ be the solution map associated with linear reaction-diffusion equation

$$\frac{\partial u}{\partial t} = D_M \frac{\partial^2 u}{\partial x^2} + (1+\epsilon) f'(0) u, \qquad 0 < t \le 1.$$

Consider the following perturbed system

$$\begin{cases} \dfrac{\partial u}{\partial t} = D_M \dfrac{\partial^2 u}{\partial x^2} + (1+\epsilon) f'(0) u, & 0 < t \leq 1,\ t \neq \tau,\ x \in \mathbb{R}, \\ u(t^+, x) = u(t,x) + \overline{\mathcal{R}}^{\epsilon}(x; N_n), & t = \tau, \\ u(0,x) = N_n(x), & n = 0, 1, 2, \ldots \\ N_{n+1}(x) = u(1,x), & \end{cases} \tag{3.3}$$

where $\overline{\mathcal{R}}^{\epsilon}(x; N_n) = (1-\epsilon) e^{-d_I \tau} g'(0) \int_{\mathbb{R}} \Gamma(D_I \tau, x-y) N_n(y) dy$. Let M^{ϵ} be the time-one solution map of (3.3), that is,

$$M^{\epsilon}[\varphi](x) := L^{\epsilon}_{1-\tau}[L^{\epsilon}_{\tau}(\varphi) + (1-\epsilon) e^{-d_I \tau} g'(0) \int_{\mathbb{R}} \Gamma(D_I \tau, \cdot - y) \varphi(y) dy](x), \quad \forall \varphi \in \mathcal{C}.$$

For any given $N_0(x) = \alpha e^{-\mu x}$ with $\mu > 0$ and $\alpha \in \mathbb{R}$, we have

$$\begin{aligned} M^0[N_0](x) :&= L^0_{1-\tau}[L^0_{\tau}(\alpha e^{-\mu \cdot}) + e^{-d_I \tau} g'(0) \alpha \int_{\mathbb{R}} \Gamma(D_I \tau, \cdot - y) e^{-\mu y} dy](x) \\ &= L^0_{1-\tau}[\alpha \underbrace{(e^{f'(0)\tau + D_M \tau \mu^2} + g'(0) e^{-d_I \tau + D_I \tau \mu^2})}_{=\Delta} e^{-\mu \cdot}](x) \\ &= \alpha \Delta e^{f'(0)(1-\tau)} \int_{\mathbb{R}} \Gamma(D_M(1-\tau), y) e^{-\mu(x-y)} dy \\ &= \alpha \Delta e^{f'(0)(1-\tau) + D_M(1-\tau)\mu^2} e^{-\mu x} \\ &= (e^{f'(0) + D_M \mu^2} + g'(0) e^{f'(0)(1-\tau) - d_I \tau + D_I \tau \mu^2 + D_M(1-\tau)\mu^2}) \alpha e^{-\mu x}. \end{aligned}$$

Following [18], we define $B_\mu : \mathbb{R} \to \mathbb{R}$ as

$$B_\mu[\alpha] = M^0[\alpha e^{-\mu x}](0) = (e^{f'(0) + D_M \mu^2} + g'(0) e^{f'(0)(1-\tau) - d_I \tau + D_I \tau \mu^2 + D_M(1-\tau)\mu^2}) \alpha, \ \forall \alpha \in \mathbb{R}.$$

Then the principle eigenvalue $\lambda(\mu)$ of B_μ can be expressed as

$$\lambda(\mu) = e^{f'(0) + D_M \mu^2} + g'(0) e^{f'(0)(1-\tau) - d_I \tau + D_I \tau \mu^2 + D_M(1-\tau)\mu^2}.$$

Let $\Phi(\mu) := \frac{\ln \lambda(\mu)}{\mu} = D_M \mu + \frac{\ln(e^{f'(0)} + g'(0) e^{f'(0)(1-\tau) - d_I \tau + D_I \tau \mu^2 - D_M \tau \mu^2})}{\mu}$. Then we have the following formula on the spreading speed c^*.

Proposition 3.1. $c^* = \inf_{\mu > 0} \Phi(\mu)$.

Proof. Clearly, $\hat{S}'(0) > 1$ implies $\lambda(0) > 1$ and $\Phi(\infty) = \infty$. Assumptions (H1) and (H2) imply that $f(u)$ and $g(u)$ are subhomogeneous, and hence,

$$f(u) \leq f'(0) u \quad \text{and} \quad g(u) \leq g'(0) u, \quad \forall u \in [0, \infty).$$

By the comparison principle, we get $Q[\phi] \leq M^0[\phi]$ for any $\phi \in \mathcal{C}_\beta$. As a result, [18, Theorem 3.10(i)] implies that $c^* \leq \inf_{\mu > 0} \Phi(\mu)$.

For given $\epsilon \in (0,1)$, there exists $\delta = \delta(\epsilon)$ such that

$$g(u) \geq (1-\epsilon)g'(0)u \quad \text{and} \quad f(u) \geq (1+\epsilon)f'(0)u, \quad \forall u \in [0,\delta].$$

Choose a positive number $\xi = \xi(\delta) > 0$ such that for any $\varphi \in \mathcal{C}_\xi$, we have

$$0 \leq u(t,x,\varphi) \leq u(t,x,\xi) < \delta, \qquad \forall (t,x) \in [0,1] \times \mathbb{R},$$

where $u(t,x,\psi)$ is a solution of (2.4) through ψ. Furthermore, the comparison principle implies that

$$Q[\varphi] \geq M^\epsilon[\varphi], \quad \forall \varphi \in \mathcal{C}_\xi.$$

By the arguments similar to those for M^0 and [18, Theorem 3.10(ii)], it follows that

$$\begin{aligned} c^* &\geq \inf_{\mu>0} \Phi^\epsilon(\mu) \\ &= \inf_{\mu>0} \Big[D_M\mu + \frac{\ln(e^{(1+\epsilon)f'(0)} + (1-\epsilon)g'(0)e^{(1+\epsilon)f'(0)(1-\tau)-d_I\tau+D_I\tau\mu^2-D_M\tau\mu^2})}{\mu} \Big]. \end{aligned}$$

Therefore, $\inf_{\mu>0}\Phi^\epsilon(\mu) \leq c^* \leq \inf_{\mu>0}\Phi(\mu)$ for all $\epsilon \in (0,1)$. Letting $\epsilon \to 0$, we then have $c^* = \inf_{\mu>0}\Phi(\mu)$. □

Definition 3.1. *The solution $N_n(x)$ is called a traveling wave solution of the recursion* (2.6) *if there exist a one-variable function w and a constant c such that $N_n(x) = w(x-cn)$ for all integers n.*

The following result on traveling wave solutions can be inferred directly from [18, Theorems 4.1 and 4.2].

Theorem 3.2. *For any $c \geq c^*$, system* (2.6) *admits a traveling wave solution $w(x-cn)$ connecting β to* 0 *such that $w(\xi)$ is nonincreasing in ξ, and for any $c \in (0,c^*)$, system* (2.6) *has no such traveling wave solution connecting β to 0.*

3.2 Scenario 2: g is not monotonically increasing

In the case where the birth function $g(N)$ is not monotonically increasing for all N, the time-one solution map Q is not monotone on its whole domain. To overcome this difficulty, we make an additional assumption on function g:

(H4) There is $\sigma > 0$ such that $g(N)$ is nondecreasing for $0 \leq N \leq \sigma$.

This assumption is reasonable biologically since it excludes the possibility of the Allee effect in the birth function where the species suffers a decrease of its fitness when the density is low [27]. For this scenario, we define

$$g^+(N) = \max_{0\leq V\leq N} g(V), \quad \forall N \geq 0.$$

One sees that g^+ is nondecreasing, locally Lipschitz continuous, and $(g^+)'(0) = g'(0)$. In the case where $\hat{S}'(0) > 1$, Lemma 3.1 implies that (3.2) with g replaced by g^+ has a positive fixed point β^+. Similarly, if we introduce

$$g^-(N) = \min_{N \le V \le \beta^+} g(V), \quad \forall 0 \le N \le \beta^+,$$

then $g^-(N)$ is nondecreasing, locally Lipschitz continuous, and equation (3.2) with g replaced by g^- admits a positive equilibrium β^-. Clearly, $0 < \beta^- \le \beta \le \beta^+$. Moreover, $g^-(N) \le g(N) \le g^+(N)$, $(g^\pm)'(0) = g'(0)$, $g^\pm(N) \le g'(0)N$, and there exists $\sigma_0 \in (0, \sigma^*]$ with $\sigma^* = \min\{\sigma, \sigma_g\}$ such that $g^\pm(N) = g(N)$ for $N \in (0, \sigma_0]$.

We now consider two auxiliary systems:

$$\begin{cases} \dfrac{\partial u}{\partial t} = D_M \dfrac{\partial^2 u}{\partial x^2} + f(u), & 0 < t \le 1, t \ne \tau, x \in \mathbb{R}, \\ u(t^+, x) = u(t, x) + \mathcal{R}^+(x; N_n^+), & t = \tau, \\ u(0, x) = N_n^+(x), & n = 0, 1, 2, \ldots \\ N_{n+1}^+(x) = u(1, x), & \end{cases} \tag{3.4}$$

and

$$\begin{cases} \dfrac{\partial u}{\partial t} = D_M \dfrac{\partial^2 u}{\partial x^2} + f(u), & 0 < t \le 1, t \ne \tau, x \in \mathbb{R}, \\ u(t^+, x) = u(t, x) + \mathcal{R}^-(x; N_n^-), & t = \tau, \\ u(0, x) = N_n^-(x), & n = 0, 1, 2, \ldots \\ N_{n+1}^-(x) = u(1, x), & \end{cases} \tag{3.5}$$

where

$$\mathcal{R}^\pm(x; N_n^\pm) = \Big(T_\tau g^\pm(N_n^\pm(\cdot))\Big)(x) = e^{-d_I \tau} \int_{\mathbb{R}} \Gamma(D_I \tau, x - y) g^\pm(N_n^\pm(y)) dy.$$

Similar to the procedures of formulating the recursion operator Q in (2.5), systems (3.4) and (3.5) define two recurrence relations for $N_n^+(x)$ and $N_n^-(x)$ as

$$N_{n+1}^+(x) = Q^+[N_n^+](x) = M_{1-\tau}[M_\tau(N_n^+) + T_\tau g^+(N_n^+)](x), \quad x \in \mathbb{R},\ n \ge 0, \tag{3.6}$$

and

$$N_{n+1}^-(x) = Q^-[N_n^-](x) = M_{1-\tau}[M_\tau(N_n^-) + T_\tau g^-(N_n^-)](x), \quad x \in \mathbb{R},\ n \ge 0, \tag{3.7}$$

respectively. Let $N_n^+(x)$, $N_n^-(x)$ and $N_n(x)$ be the solutions of (3.6), (3.7) and (2.6), respectively. The comparison arguments show that if $N_0^-(x) \le N_0(x) \le N_0^+(x) \le \beta^+$, then

$$0 \le N_n^-(x) \le N_n(x) \le N_n^+(x), \quad x \in \mathbb{R},\ n \ge 0.$$

Note that $c^* = \inf_{\mu>0} \Phi(\mu)$ in Subsection 3.1 is the spreading speed of (2.6) with monotone birth rate function, and the expression of c^* only depends on the linearized equation at $u = 0$. Based on this fact, we can define same $(c^+)^*$ and $(c^-)^*$ for (3.6) and (3.7), respectively in a similar manner. Moreover, $(c^-)^* = (c^+)^*$. With the help of two systems (3.4) and (3.5), we can use the comparison arguments similar to those in [10, Theorem 2.2] to prove the following result, which implies that $c^* = (c^-)^* = (c^+)^*$ is also a spreading speed for system (2.6).

Theorem 3.3. *Suppose* $\hat{S}'(0){=}e^{f'(0)} + g'(0)e^{f'(0)(1-\tau)-d_I\tau}{>}\, 1$ *and assumptions (H1)-(H4) hold. Then the following statements are valid:*

(i) For any $c > c^*$*, if* $\phi \in \mathcal{C}_{\beta+}$ *with* $0 \le \phi \ll \beta^+$ *and* $\phi(\cdot) = 0$ *outside a bounded interval, then* $\lim_{n\to\infty, |x|\ge cn} Q^n[\phi](x) = 0$.

(ii) For any $c < c^*$*, if* $\phi \in \mathcal{C}_{\beta+} \setminus \{0\}$*, then*

$$\beta^- \le \liminf_{n\to\infty, |x|\le cn} Q^n[\phi](x) \le \limsup_{n\to\infty, |x|\le cn} Q^n[\phi](x) \le \beta^+.$$

In order to address traveling waves for system (2.6), we define the operators

$$Q_c[u](x) := \hat{T}_c Q[u](x) = \hat{T}_c\{M_{1-\tau}[M_\tau(u) + T_\tau g(u)]\}(x),$$

and

$$Q_c^{\pm}[u](x) := \hat{T}_c Q^{\pm}[u](x) = \hat{T}_c\{M_{1-\tau}[M_\tau(u) + T_\tau g^{\pm}(u)]\}(x),$$

where $\hat{T}_c[u](x) = u(x+c)$ for $x \in \mathbb{R}$. Since the operators $Q^{\pm}$ are order-preserving, Theorem 3.2 implies that for all $c \ge c^*$, (3.6) and (3.7) admit nontrivial nonincreasing traveling waves $w^+(x - nc)$ and $w^-(x - nc)$, respectively, with $w^{\pm}(+\infty) = 0$ and $w^{\pm}(-\infty) = \beta^{\pm}$.

For a given $\rho > 0$, define

$$X_\rho := \{\phi \in C(\mathbb{R}, \mathbb{R}) : \sup_{x\in\mathbb{R}} |\phi(x)| e^{-\rho|x|} < +\infty\},$$

and $\|\phi\|_\rho := \sup\limits_{x\in\mathbb{R}} |\phi(x)| e^{-\rho|x|}$. It then follows that $(X_\rho, \|\cdot\|_\rho)$ is a Banach space. For any $c \ge c^*$, let

$$E_c = \{u \in X_\rho : \delta w^+(x) \le u(x) \le w^+(x),\ x \in \mathbb{R}\}$$

with $0 < \delta < 1$ and $\delta w^+(x) \le \sigma_0$. Clearly, E_c is a nonempty, bounded, closed and convex subset of X_ρ. Further, we have the following two properties for the operator Q_c.

Lemma 3.2. *The operator* Q_c *maps* E_c *into* E_c.

Proof. Note that $g^+ \geq g$ and g^+ is nondecreasing. If $u \leq w^+$, then

$$Q_c[u] \leq Q_c^+[u] \leq Q_c^+[w^+] = w^+.$$

On the other hand, if $u \geq \delta w^+$, then

$$\begin{aligned} Q_c[u] \geq Q_c^-[u] \geq Q_c^-[\delta w^+] & \\ &= \hat{T}_c\{M_{1-\tau}[M_\tau(\delta w^+) + T_\tau g^-(\delta w^+)]\} \\ &\geq \delta \hat{T}_c\{M_{1-\tau}[M_\tau(w^+) + T_\tau g^+(w^+)]\} \\ &= \delta Q_c^+[w^+] = \delta w^+. \end{aligned}$$

Here we have used the fact that $g^-(\delta w^+) = g^+(\delta w^+) \geq \delta g^+(w^+)$. Thus, the desired result follows. □

Lemma 3.3. *The map $Q_c : E_c \to E_c$ is continuous and compact with respect to $\| \cdot \|_\rho$.*

Proof. For any ϕ_1, $\phi_2 \in E_c$ and $t \in [0, \tau]$, we let $M_t(\phi_i)(x) = u(t, x, \phi_i)$, $x \in \mathbb{R}$, $i = 1, 2$. Then

$$\begin{aligned} & |u(t, x, \phi_1) - u(t, x, \phi_2)| e^{-\rho|x|} \\ \leq & \int_{\mathbb{R}} \Gamma(D_M t, y) |\phi_1(x - y) - \phi_2(x - y)| e^{-\rho|x|} dy \\ & + \int_0^t \int_{\mathbb{R}} \Gamma(D_M(t - s), y) L_f |u(s, x - y, \phi_1) - u(s, x - y, \phi_2)| e^{-\rho|x|} dy ds \\ \leq & \|\phi_1 - \phi_2\|_\rho \int_{\mathbb{R}} \Gamma(D_M t, y) e^{\rho|y|} dy \\ & + \int_0^t \|u(s, \cdot, \phi_1) - u(s, \cdot, \phi_2)\|_\rho L_f \int_{\mathbb{R}} \Gamma(D_M(t - s), y) e^{\rho|y|} dy ds \\ \leq & \|\phi_1 - \phi_2\|_\rho 2 e^{\rho^2 D_M \tau} + \int_0^t \|u(s, \cdot, \phi_1) - u(s, \cdot, \phi_2)\|_\rho 2 L_f e^{\rho^2 D_M (t-s)} ds, \end{aligned}$$

where L_f is the Lipschitz constant of f on $[0, \beta^+]$ and we have used the fact that $\int_{\mathbb{R}} \Gamma(D_M t, y) e^{\rho|y|} dy \leq 2 e^{\rho^2 D_M t}$ for all $t \geq 0$. By Gronwall's inequality, it then follows that

$$\|u(t, \cdot, \phi_1) - u(t, \cdot, \phi_2)\|_\rho \leq 2 e^{\rho^2 D_M \tau + \frac{2L_f}{\rho^2 D_M}(e^{\rho^2 D_m t} - 1)} \|\phi_1 - \phi_2\|_\rho,$$

and hence,

$$\|M_\tau(\phi_1) - M_\tau(\phi_2)\|_\rho \leq 2 e^{\rho^2 D_M \tau + \frac{2L_f}{\rho^2 D_M}(e^{\rho^2 D_m \tau} - 1)} \|\phi_1 - \phi_2\|_\rho.$$

This implies that M_τ is continuous on E_c. Similarly, we can prove the continuity of $\hat{T}_c, T_\tau g$ and $M_{1-\tau}$ with respect to $\| \cdot \|_\rho$. Therefore, $Q_c : E_c \to E_c$ is continuous.

Next we prove that $Q_c[E_c]$ is precompact in X_ρ. For this purpose, we first show that for any given $t \in (0, \tau]$, the map $M_t : \mathcal{C}_{\beta+} \to \mathcal{C}_{\beta+}$ is compact with respect to the compact open topology. Let $U(t)$ be the solution semigroup generated by

$$\begin{cases} \dfrac{\partial v}{\partial t} = D_M \dfrac{\partial^2 v}{\partial x^2}, \quad t > 0, \ x \in \mathbb{R}, \\ v(0, \cdot) = \varphi \in \mathcal{C}. \end{cases}$$

Then

$$[U(t)\varphi](x) = \int_{\mathbb{R}} \Gamma(D_M t, y)\varphi(x - y)dy = \int_{\mathbb{R}} \Gamma(D_M t, x - y)\varphi(y)dy.$$

Let B be any given bounded subset of $\mathcal{C}_{\beta+}$. For any $\varphi \in B, x_1, x_2 \in \mathbb{R}$, we have

$$\begin{aligned} &|[U(t)\varphi](x_1) - [U(t)\varphi](x_2)| \\ &= \left| \int_{\mathbb{R}} \left(\Gamma(D_M t, x_1 - y) - \Gamma(D_M t, x_2 - y)\right) \varphi(y)dy \right| \\ &\leq \beta^+ \int_{\mathbb{R}} |\Gamma(D_M t, x_1 - x_2 + z) - \Gamma(D_M t, z)| \, dz \to 0 \ \ (\text{as } |x_1 - x_2| \to 0). \end{aligned}$$

Thus, the family of functions $\{[U(t)\varphi](x) : \varphi \in B\}$ is both uniformly bounded and equicontinuous in $x \in \mathbb{R}$. By the Arzela-Ascoli theorem, it then follows that for every sequence φ_n in B, there exists a subsequence φ_{n_k} such that $[U(t)\varphi_{n_k}](x)$ converges to a function in $\mathcal{C}_{\beta+}$ uniformly for x in any compact subset of $\mathbb{R}$. This implies that the set $U(t)B$ is precompact in $\mathcal{C}_{\beta+}$.

By the constant-variation formula, for any $\epsilon \in (0, t)$, $t \in (0, \tau]$ and $\phi \in \mathcal{C}_{\beta+}$, we have

$$\begin{aligned} &M_t(\phi) = u(t, \cdot, \phi) \\ &= U(t)\phi + \int_0^{t-\epsilon} U(t - s)f(u(s, \cdot, \phi))ds + \int_{t-\epsilon}^t U(t - s)f(u(s, \cdot, \phi))ds \\ &= U(\epsilon) \left[U(t - \epsilon)\phi + \int_0^{t-\epsilon} U(t - \epsilon - s)f(u(s, \cdot, \phi))ds \right] + \int_{t-\epsilon}^t U(t - s)f(u(s, \cdot, \phi))ds \\ &= U(\epsilon)u(t - \epsilon, \cdot, \phi) + \int_{t-\epsilon}^t U(t - s)f(u(s, \cdot, \phi))ds. \end{aligned}$$

Since $\{u(t - \epsilon, \phi) : \phi \in \mathcal{C}_{\beta+}\}$ is bounded in $\mathcal{C}$ and $U(\epsilon)$ is compact, we have

$$\hat{\alpha}(\{U(\epsilon)u(t - \epsilon, \cdot, \phi) : \phi \in \mathcal{C}_{\beta+}\}) = 0,$$

where $\hat{\alpha}$ is the Kuratowski measure of noncompactness in $(\mathcal{C}, \| \cdot \|_{\mathcal{C}})$. Moreover, it is easy to see that $\{U(t - s)f(u(s, \cdot, \phi)) : \phi \in \mathcal{C}_{\beta+}\}$ is bounded in $\mathcal{C}$ and for each $t \in (0, \tau]$, there exists $H_t > 0$ such that

$$\left\| \int_{t-\epsilon}^t U(t - s)f(u(s, \cdot, \phi))ds \right\|_{\mathcal{C}} \leq H_t \epsilon, \quad \forall \phi \in \mathcal{C}_{\beta+}.$$

By virtue of the fact $\hat{\alpha}(A) \leq d(A)$, where $d(A)$ is the diameter of $A \subseteq \mathcal{C}$, we obtain

$$\hat{\alpha}\left(\left\{\int_{t-\epsilon}^{t} U(t-s)f(u(s,\cdot,\phi))ds : \phi \in \mathcal{C}_{\beta^+}\right\}\right) \leq 2H_t\epsilon, \quad \forall t \in (0,\tau].$$

It then follows that

$$\begin{aligned}
&\hat{\alpha}(\{u(t,\cdot,\phi) : \phi \in \mathcal{C}_{\beta^+}\}) \\
&\leq \hat{\alpha}(\{U(\epsilon)u(t-\epsilon,\cdot,\phi) : \phi \in \mathcal{C}_{\beta^+}\}) + \hat{\alpha}\left(\left\{\int_{t-\epsilon}^{t} U(t-s)f(u(s,\cdot,\phi))ds : \phi \in \mathcal{C}_{\beta^+}\right\}\right) \\
&\leq 2H_t\epsilon, \quad \forall t \in (0,\tau].
\end{aligned}$$

Letting $\epsilon \to 0$, we have $\hat{\alpha}(\{u(t,\cdot,\phi) : \phi \in \mathcal{C}_{\beta^+}\}) = 0$, and hence, for each $t \in (0,\tau]$, $M_t(\mathcal{C}_{\beta^+})$ is precompact with respect to the compact open topology.

The compactness of $T_\tau g$ and $M_{1-\tau}$ with respect to the compact open topology can be proved similarly. Since $\hat{T}_c$ is continuous and $Q[\cdot] = M_{1-\tau}[M_\tau(\cdot) + T_\tau g(\cdot)]$ is compact, the composition operator $Q_c = \hat{T}_c Q$ is also compact. It then follows that for any given sequence $\{\psi_n := Q_c[\phi_n]\}_{n\geq 1} \subset Q_c[E_c]$, there exists $n_k \to \infty$ and $\psi \in C(\mathbb{R},\mathbb{R})$ such that $\lim_{k\to\infty} \psi_{n_k}(x) = \psi(x)$ uniformly for x in any compact subset of $\mathbb{R}$. Since ψ_{n_k} is bounded by δw^+ and w^+, so is the limit ψ. This implies that $\psi \in E_c$. Moreover, for any $\bar{\epsilon} > 0$, there exists a $K > 0$ such that

$$|\psi_{n_k}(x) - \psi(x)|e^{-\rho|x|} \leq w^+(x)e^{-\rho|x|} < \bar{\epsilon}, \quad \forall |x| \geq K, \ k \geq 1.$$

On the other hand, it follows from the uniform convergence of $\psi_{n_k}(x)$ on $[-K,K]$ that there exists an integer k_0 such that

$$|\psi_{n_k}(x) - \psi(x)|e^{-\rho|x|} < \bar{\epsilon}, \quad \forall |x| \leq K, \ k \geq k_0.$$

From the above two inequalities, we see that $\psi_{n_k} \to \psi$ in E_c with respect to the norm $\|\cdot\|_\rho$. This shows that $Q_c : E_c \to E_c$ is compact. □

Now we are ready to prove the existence of traveling wave solutions.

Theorem 3.4. *Suppose* $\hat{S}'(0)=e^{f'(0)} + g'(0)e^{f'(0)(1-\tau)-d_I\tau} > 1$ *and assumptions (H1)-(H4) hold. Then the following statements are valid:*

(i) For any $c \in (0,c^*)$, *system* (2.6) *has no traveling wave in the form of* $w(x-cn)$ *with* $w(+\infty) = 0$.

(ii) For any $c \geq c^*$, *system* (2.6) *has a continuous traveling wave in the form of* $w(x-cn)$ *such that* $w(+\infty) = 0$ *and* $\beta^- \leq \liminf_{\xi\to-\infty} w(\xi) \leq \limsup_{\xi\to-\infty} w(\xi) \leq \beta^+$.

Proof. Statement (i) can be proved by the arguments similar to those in the first part of the proof of [32, Theorem 3.5(i)]. By Lemma 3.2, Lemma 3.3 and Schauder's fixed point theorem, it follows that there exists $w \in E_c$ such that $Q_c[w](x) = w(x)$ for all $x \in \mathbb{R}$. Hence, $Q[w](x) = w(x-c)$ and $Q^n[w](x) = w(x-cn)$ is a traveling wave solution of (2.6). Since $\delta w^+(\xi) \le w(\xi) \le w^+(\xi), \xi = x - c$, we have $w(+\infty) = 0$.

For a fixed $c \ge c^*$, let $u_n(x) = w(x-cn)$, $\forall n \ge 0$ be a wave profile. Fix $\bar{c} \in (0, c^*)$, it follows from Theorem 3.3(ii) that

$$\beta^- \le \liminf_{n\to\infty, |x|\le \bar{c}n} u_n(x) \le \limsup_{n\to\infty, |x|\le \bar{c}n} u_n(x) \le \beta^+,$$

and hence,

$$\beta^- \le \liminf_{n\to\infty} u_n(kn) \le \limsup_{n\to\infty} u_n(kn) \le \beta^+ \text{ uniformly for } k \in [0, \bar{c}].$$

This implies that $\beta^- \le \liminf_{n\to\infty} w(sn) \le \limsup_{n\to\infty} w(sn) \le \beta^+$ uniformly for $s \in [-c, \bar{c} - c]$. Let $a_n = -cn$, $b_n = (\bar{c} - c)n$, $\forall n \ge 1$. Then there exists $j_0 > 0$ such that $a_n \le b_{n+1}$, $\forall n \ge j_0$, and hence, $\cup_{n\ge j}[a_n, b_n] = (-\infty, b_{j_0}]$, $\forall j \ge j_0$. Consequently, we obtain that $\beta^- \le \liminf_{\xi\to-\infty} w(\xi) \le \limsup_{\xi\to-\infty} w(\xi) \le \beta^+$. □

4 Critical domain size

In this section, we consider the model in a bounded spatial domain $[0, L]$ and discuss the values of L that can support the species establishment in this domain. Assume that the boundary is hostile for the species, and therefore, Dirichelet boundary condition can be imposed for the species density variable $u(t, x)$ at time t of a specific year at location x.

Following the model formulation procedures for system (2.4), we can derive the system for the population growth on a bounded domain $[0, L]$:

$$\begin{cases} \dfrac{\partial u}{\partial t} = D_M \dfrac{\partial^2 u}{\partial x^2} + f(u), & 0 < t \le 1,\ t \ne \tau,\ 0 < x < L, \\ u(t^+, x) = u(t, x) + \mathcal{R}(x; N_n), & t = \tau, \\ u(0, x) = N_n(x), & n = 0, 1, 2, \ldots \\ u(t, 0) = u(t, L) = 0, & \\ N_{n+1}(x) = u(1, x). & \end{cases} \tag{4.1}$$

Please note that the initial condition for model (4.1) is $u(0, x) = N_0(x)$, $\forall x \in (0, L)$. The impulsive perturbation term to account for the synchronized maturation should be reformulated as

$$\mathcal{R}(x; N_n) = e^{-d_I \tau} \int_0^L \tilde{\Gamma}(D_I \tau, x, y) g(N_n(y)) dy$$

with $\tilde{\Gamma}(t,x,y)$ being the Green function associated with the operator $\partial_t - \triangle$ subject to the Dirichlet boundary condition on the domain $[0,L]$. As discussed in Section 3, we introduce a discrete-time recursion:

$$N_{n+1}(x) = \mathcal{Q}[N_n](x) = \mathcal{M}_{1-\tau}[\mathcal{M}_\tau(N_n) + \mathcal{T}_\tau g(N_n)](x), \quad x \in [0,L],\ n \geq 0, \tag{4.2}$$

which will be used to investigate the spatial dynamics of model (4.1). Here $\mathcal{T}_t$ and $\mathcal{M}_t$ are the solution maps of the following tow equations:

$$\frac{\partial v}{\partial t} = D_I \frac{\partial^2 v}{\partial x^2} - d_I v \ \text{ and } \ \frac{\partial u}{\partial t} = D_M \frac{\partial^2 u}{\partial x^2} + f(u), \quad t > 0,\ x \in (0,L)$$

with the Dirichlet boundary condition, respectively. In next two subsections, we are going to discuss the critical domain size problem for two different scenarios: (i) the birth function g is monotonically increasing, and (ii) the birth function g is not monotone.

4.1 Scenario 1: The birth function g is monotone

Consider two Dirichlet eigenvalue problems

$$\begin{cases} D_M \dfrac{d^2\phi}{dx^2} + f'(0)\phi = \lambda\phi, & 0 < x < L, \\ \phi(0) = \phi(L) = 0, \end{cases} \tag{4.3}$$

and

$$\begin{cases} D_I \dfrac{d^2\phi}{dx^2} - d_I\phi = \lambda\phi, & 0 < x < L, \\ \phi(0) = \phi(L) = 0. \end{cases} \tag{4.4}$$

It is easily seen that $\lambda_1 = f'(0) - \frac{D_M\pi^2}{L^2}$ and $\lambda_2 = -d_I - \frac{D_I\pi^2}{L^2}$ are the principal eigenvalues of (4.3) and (4.4), respectively with the same eigenfunction $\phi_*(x) = \sin\frac{\pi x}{L}$. To obtain the critical domain size of (4.2), we introduce a function

$$\begin{aligned} h(L) &= e^{\lambda_1} + g'(0)e^{\lambda_1(1-\tau)+\lambda_2\tau} \\ &= e^{f'(0)-\frac{D_M\pi^2}{L^2}} + g'(0)e^{f'(0)(1-\tau)-\frac{D_M\pi^2(1-\tau)}{L^2}-d_I\tau-\frac{D_I\pi^2\tau}{L^2}}. \end{aligned}$$

It is easy to check that this function admits the following properties: (i) $\lim_{L\to 0} h(L) = 0$, (ii) $h_\infty := \lim_{L\to\infty} h(L) = e^{f'(0)} + g'(0)e^{f'(0)(1-\tau)-d_I\tau}$ and (iii) $h'(L) > 0$ for $L \in (0,\infty)$. Therefore, if $h_\infty > 1$, there is a unique $L^* > 0$ such that $h(L^*) = 1$.

To establish a threshold-type result on the global dynamics for system (4.2), we first need the following result.

Lemma 4.1. *If $h_\infty > 1$ and $L > L^*$, then $\epsilon\phi_*(x)$ is a subsolution of the map $\mathcal{Q}$ for small $\epsilon > 0$.*

Proof. In this case, we have $h(L) > 1$, and therefore, we can choose $\hat{\lambda}_1 < \lambda_1$ and $\gamma \in (0, g'(0))$ such that $e^{\hat{\lambda}_1} + e^{\hat{\lambda}_1(1-\tau)+\lambda_2\tau}\gamma > 1$. Let

$$z(t,x) = \begin{cases} \epsilon e^{\hat{\lambda}_1 t}\phi_*(x), & 0 \le t \le \tau, \\ \epsilon e^{\hat{\lambda}_1(t-\tau)}[e^{\hat{\lambda}_1\tau} + e^{\lambda_2\tau}\gamma]\phi_*(x), & \tau < t \le 1. \end{cases}$$

By (H3), for sufficiently small $\epsilon > 0$, we have

$$\begin{aligned} &\frac{\partial z}{\partial t} - D_M\frac{\partial^2 z}{\partial x^2} - f(z) \\ \le&\epsilon\hat{\lambda}_1 e^{\hat{\lambda}_1 t}\phi_* - D_M\epsilon e^{\hat{\lambda}_1 t}\phi_*'' - \epsilon e^{\hat{\lambda}_1 t}\phi_* f'(0) + F(\epsilon e^{\hat{\lambda}_1 t}\phi_*)^{\nu_f} \\ =&\epsilon e^{\hat{\lambda}_1 t}[\hat{\lambda}_1\phi_* - D_M\phi_*'' - f'(0)\phi_*] + F(\epsilon e^{\hat{\lambda}_1 t}\phi_*)^{\nu_f} \\ =&z[\hat{\lambda}_1 - \lambda_1 + F\epsilon^{\nu_f - 1}(e^{\hat{\lambda}_1 t}\phi_*)^{\nu_f - 1}] \le 0, \quad 0 < t \le \tau, \end{aligned}$$

and

$$\begin{aligned} &\frac{\partial z}{\partial t} - D_M\frac{\partial^2 z}{\partial x^2} - f(z) \\ \le&\epsilon\hat{\lambda}_1 e^{\hat{\lambda}_1(t-\tau)}\mathcal{K}\phi_* - D_M\epsilon e^{\hat{\lambda}_1(t-\tau)}\mathcal{K}\phi_*'' - \epsilon e^{\hat{\lambda}_1(t-\tau)}\mathcal{K}\phi_* f'(0) + F(\epsilon e^{\hat{\lambda}_1(t-\tau)}\mathcal{K}\phi_*)^{\nu_f} \\ =&\epsilon e^{\hat{\lambda}_1(t-\tau)}\mathcal{K}[\hat{\lambda}_1\phi_* - D_M\phi_*'' - f'(0)\phi_*] + F(\epsilon e^{\hat{\lambda}_1(t-\tau)}\mathcal{K}\phi_*)^{\nu_f} \\ =&z[\hat{\lambda}_1 - \lambda_1 + F\epsilon^{\nu_f - 1}(e^{\hat{\lambda}_1(t-\tau)}\mathcal{K}\phi_*)^{\nu_f - 1}] \le 0, \quad \tau < t \le 1, \end{aligned}$$

where $\mathcal{K} = e^{\hat{\lambda}_1\tau} + e^{\lambda_2\tau}\gamma$. This shows that $z(t,x)$ is a lower solution of

$$\begin{cases} \dfrac{\partial u}{\partial t} = D_M\dfrac{\partial^2 u}{\partial x^2} + f(u), \quad 0 < t \le 1, \ t \ne \tau, \ 0 < x < L, \\ u(t,0) = u(t,L) = 0. \end{cases}$$

Moreover, for the above $\epsilon > 0$, assumption (H3) implies that

$$g(\epsilon\phi_*) \ge g'(0)\epsilon\phi_* - G(\epsilon\phi_*)^{\nu_g} = \gamma\epsilon\phi_* + \epsilon\phi_*\Big(g'(0) - \gamma - G\epsilon^{\nu_g - 1}\phi_*^{\nu_g - 1}\Big) \ge \gamma\epsilon\phi_*.$$

Thus, there exists a sufficiently small ϵ_0 such that for any given $\epsilon \in (0, \epsilon_0]$, we have $\overline{M} > \epsilon\phi_*$ and

$$\begin{aligned} \mathcal{Q}[\epsilon\phi_*] &= \mathcal{M}_{1-\tau}[\mathcal{M}_\tau(\epsilon\phi_*) + \mathcal{T}_\tau g(\epsilon\phi_*)] \\ &\ge \mathcal{M}_{1-\tau}[e^{\hat{\lambda}_1\tau}\epsilon\phi_* + e^{\lambda_2\tau}\gamma\epsilon\phi_*] \ge (e^{\hat{\lambda}_1} + e^{\hat{\lambda}_1(1-\tau)+\lambda_2\tau}\gamma)\epsilon\phi_* \ge \epsilon\phi_*. \end{aligned}$$

The desired result follows. □

To consider a Dirichlet boundary condition, we choose

$$X = \{\psi \in C([0,L],\mathbb{R}) : \ \psi(0) = \psi(L) = 0\}$$

with the cone X^+ of nonnegative functions in X. Since $\mathrm{Int}(X^+)$ is empty, we further introduce the following Banach space:

$$Y = \{\varphi \in C^1([0,L],\mathbb{R}) : \ \varphi(0) = \varphi(L) = 0\}$$

with the usual norm in C^1. The set of nonnegative functions in Y forms a solid cone Y^+ with nonempty interior given by

$$\mathrm{Int}(Y^+) = \{\varphi \in Y : \ \varphi(x) > 0 \text{ for all } x \in (0,L), \varphi'(0) > 0 \text{ and } \varphi'(L) < 0\}.$$

Then we have the following result.

Theorem 4.1. *Suppose $h_\infty > 1$. Then the following statements are valid:*

(i) If $L < L^*$, then the zero steady state is globally asymptotically stable for system (4.2) *in X^+.*

(ii) If $L > L^*$, then system (4.2) *has a unique positive steady state $N_* \in Int(Y^+)$, which is global asymptotically stable with respect to initial values in $X^+ \setminus \{0\}$.*

Proof. (i) When $L < L^*$, we have $h(L) < 1$. Let $\tilde{N}_n(x) = \delta[h(L)]^n \phi_*(x)$, $n = 0, 1, 2, \dots$, where δ is a positive constant. Then $\tilde{N}_n(x)$ satisfies

$$\begin{cases} \dfrac{\partial u}{\partial t} = D_M \dfrac{\partial^2 u}{\partial x^2} + f'(0)u, & 0 < t \le 1, \ t \neq \tau, \ 0 < x < L, \\ u(t^+, x) = u(t,x) + \tilde{\mathcal{R}}(x; \tilde{N}_n), & t = \tau, \\ u(0,x) = \tilde{N}_n(x), & n = 0, 1, 2, \dots \\ u(t,0) = u(t,L) = 0, \\ \tilde{N}_{n+1}(x) = u(1,x), \end{cases}$$

where $\tilde{\mathcal{R}}(x; \tilde{N}_n) = e^{-d_I \tau} g'(0) \int_0^L \tilde{\Gamma}(D_I \tau, x, y) \tilde{N}_n(y) dy$. For any given $u(0,x) = N_0(x)$ in (4.1), one can choose a sufficiently large δ such that $N_0(x) \le \tilde{N}_0(x)$. Applying the standard comparison theorem and mathematical induction arguments, we obtain $N_n(x) \le \tilde{N}_n(x)$ for all $n \ge 0$. This implies that $\lim_{n\to\infty} N_n(x) = 0$ uniformly for $x \in [0,L]$. The desired result immediately follows from [33, Lemma 2.1].

(ii) By Lemma 4.1, we know that $\epsilon\phi_*$ is a subsolution of the map $\mathcal{Q}$. Then induction argument shows that

$$\overline{M} \ge \mathcal{Q}^{n+1}[\epsilon\phi_*](x) \ge \mathcal{Q}^n[\epsilon\phi_*](x), \qquad x \in [0,L], \ n \ge 0.$$

It is easy to see that the discrete orbit $\gamma^+(\epsilon\phi_*) = \{\mathcal{Q}^n(\epsilon\phi_*) : \ n \ge 1\}$ is precompact in X^+. Hence, there is $N_* \in X^+ \setminus \{0\}$ such that $\lim_{n\to\infty} \mathcal{Q}^n[\epsilon\phi_*](x) = N_*(x)$ uniformly for any $x \in [0, L]$, and $\mathcal{Q}N_* = N_*$. Clearly, $N_*(x) > 0$ in $(0, L)$ and $N_*(0) = N_*(L) = 0$. According to the proof of [26, Corollary 4.2], we have that $N_* \in \mathrm{Int}(Y^+)$. Moreover, if $N_{**} \in \mathrm{Int}(Y^+)$ is another fixed point of $\mathcal{Q}$. By [36, Lemma 2.3.1] with $U = \mathrm{Int}(Y^+)$, it follows that $N_* = \eta N_{**}$ for some $\eta \in (0, 1]$. We further claim $\eta = 1$, that is, $N_* = N_{**}$. Suppose otherwise that $\eta \in (0, 1)$. First we can verify that $\mathcal{Q}: \ \mathrm{Int}(Y^+) \to \mathrm{Int}(Y^+)$ is strongly subhomogeneous. Then we have

$$N_* = \mathcal{Q}(N_*) = \mathcal{Q}(\eta N_{**}) \gg_Y \eta \mathcal{Q}(N_{**}) = \eta N_{**} = N_*,$$

which leads a contradiction.

Finally, we prove that the solution $N_n(x)$ with the initial value $N_0 = \varphi \in X^+ \setminus \{0\}$ satisfies $\lim_{n\to\infty} N_n(x) = N_*(x)$, $\forall x \in [0, L]$. Arguments in the proof of [26, Corollary 4.2] imply that $N_1(\cdot) \in \mathrm{Int}(Y^+)$. Without loss of generality, we may set N_1 as the new initial datum in the space $\mathrm{Int}(Y^+)$. Then $\mathcal{Q}: \ \mathrm{Int}(Y^+) \to \mathrm{Int}(Y^+)$ is strongly monotone and strictly subhomogeneous, and [36, Theorem 2.3.2] gives rise to

$$\lim_{n\to\infty} \mathcal{Q}^{n+1}(\varphi)(x) = \lim_{n\to\infty} \mathcal{Q}^n(N_1)(x) = N_*(x)$$

uniformly for $x \in [0, L]$. By virtue of [33, Lemma 2.1], we obtain the global stability of $N_*(x)$. □

4.2 Scenario 2: g is not monotonically increasing

Now we consider the case where g is not monotone. In this case, we need an additional assumption (H4) as in subsection 3.2 to address the critical domain size problem. Recalling the definition of g^+ and g^- in subsection 3.2, we consider the following two auxiliary systems:

$$\begin{cases} \dfrac{\partial u}{\partial t} = D_M \dfrac{\partial^2 u}{\partial x^2} + f(u), & 0 < t \le 1, t \ne \tau, 0 < x < L, \\ u(t^+, x) = u(t, x) + \mathcal{R}^+(x; N_n^+), & t = \tau, \\ u(0, x) = N_n^+(x), & n = 0, 1, 2, \ldots \\ u(t, 0) = u(t, L) = 0, & \\ N_{n+1}^+(x) = u(1, x), & \end{cases} \tag{4.5}$$

and

$$\begin{cases} \dfrac{\partial u}{\partial t} = D_M \dfrac{\partial^2 u}{\partial x^2} + f(u), & 0 < t \le 1, t \ne \tau, 0 < x < L, \\ u(t^+, x) = u(t, x) + \mathcal{R}^-(x; N_n^-), & t = \tau, \\ u(0, x) = N_n^-(x), & n = 0, 1, 2, \ldots \\ u(t, 0) = u(t, L) = 0, & \\ N_{n+1}^-(x) = u(1, x), & \end{cases} \tag{4.6}$$

where

$$\mathcal{R}^{\pm}(x; N_n^{\pm}) = \Big(\mathcal{T}_\tau g^{\pm}(N_n^{\pm}(\cdot))\Big)(x) = e^{-d_I\tau}\int_0^L \tilde{\Gamma}(D_I\tau, x, y) g^{\pm}(N_n^{\pm}(y))dy.$$

Then discrete-time recursions can be well derived from (4.5) and (4.6) as a time-one solution map on a space of functions:

$$N_{n+1}^{+}(x) = \mathcal{Q}^{+}[N_n^{+}](x) = \mathcal{M}_{1-\tau}[\mathcal{M}_\tau(N_n^{+}) + \mathcal{T}_\tau g^{+}(N_n^{+})](x), \quad x \in [0, L],\ n \geq 0, \tag{4.7}$$

and

$$N_{n+1}^{-}(x) = \mathcal{Q}^{-}[N_n^{-}](x) = \mathcal{M}_{1-\tau}[\mathcal{M}_\tau(N_n) + \mathcal{T}_\tau g^{-}(N_n^{-})](x), \quad x \in [0, L],\ n \geq 0. \tag{4.8}$$

The comparison principle shows that if $0 < N_0^{-}(x) \leq N_0(x) \leq N_0^{+}(x) \leq \beta^{+}$, then

$$0 \leq N_n^{-}(x) \leq N_n(x) \leq N_n^{+}(x) \leq \beta^{+}, \quad x \in [0, L],\ n \geq 0. \tag{4.9}$$

Following same arguments as in the previous subsection 4.1, we can show that systems (4.5) and (4.6), with increasing birth functions g^{+} and g^{-} respectively, admit critical domain sizes, and moreover, the critical domain sizes for systems (4.5) and (4.6) are consistent. By using this observation and (4.9), combined with the arguments in the previous subsection, we can easily obtain the following result.

Theorem 4.2. *When the birth function g is not monotone, but an additional assumption (H4) holds, the following statements are valid:*

(i) If $L < L^*$, then the zero steady state is globally attractive for system (4.2) in X^{+}.

(ii) If $L > L^*$, then the solution sequence $N_n(x)$ of system (4.2) with initial data $N_0 \in X^{+} \setminus \{0\}$ satisfies

$$\limsup_{n\to\infty} \max_{x\in[0,L]} [N_n(x) - N_*^{+}(x)] \leq 0 \leq \liminf_{n\to\infty} \min_{x\in[0,L]} [N_n(x) - N_*^{-}(x)],$$

where $N_*^{-}(x)$ and $N_*^{+}(x)$ are positive steady states of systems (4.8) and (4.7), respectively.

5 Numerical simulations and discussions

In this paper, we formulate an impulsive reaction-diffusion population growth model with a maturation pulse, which was motivated by annually synchronized emergence of adults. Through carefully compositing a time-τ map in interval $[0, \tau]$ with impulsive maturation, and a time-$(1-\tau)$ map in interval $[\tau, 1]$, a discrete-time semiflow on an infinite dimensional space is derived to account the evolution from this year's adult density distribution in a spatial domain to that of the next year. By investigating the properties of such a discrete-time semilfow, rigorous analysis is performed on the spatial dynamics of the original impulsive reaction-diffusion model. In particular, the existence of the spreading speed and the traveling waves is established when the habitat is an unbounded domain, and furthermore, it is confirmed that the spreading speed coincides with the minimal wave speed for traveling wave solutions. In the case where the spatial habitat is a one-dimensional bounded domain $[0, L]$, species persistence and extinction is shown to be determined by the domain size and the critical domain size is investigated by using the explicitly expressed principal eigenvalue of the Laplacian operator.

To verify these analytic results and to explore the effects of the adult emergence delay on the propagation dynamics, we perform illustrative numerical investigations through the backward (implicit) difference method (see [20, Section 2.1.4]) in MATLAB 2019a, which is an efficient and unconditionally stable numerical algorithm. The baseline parameter settings are taken as follows: The loss function f takes the form $f(N) = -aN - bN^2$, with $a = 1$ being the natural density-independence death rate of the population and $b = 0.01$ representing the strength of the interspecific competition between individuals [14, 32]. Two widely used types of birth functions, the Beverton-Holt function $g(N) = \frac{pN}{q+N}$ and the Ricker function $g(N) = Ne^{r-kN}$ will be employed to simulate different scenarios where g is monotone and non-monotone, respectively. Unless stated otherwise, the default parameter values are set as $p = 1.8$, $q = 0.2$ in the Beverton-Holt function, and $r = 2.5$, $k = 1$ in the Ricker function. For illustration, other parameters are fixed at $d_I = 0.5$, $D_M = 1$ and $D_I = 0.2$.

5.1 The effect of delay on the spatial spread

Taking the initial function as $N_0(x) = \cos(\frac{\pi}{20}x)$ with a compact support from -10 to 10 in the domain $[-50, 50]$, the spreading of species is illustrated in Fig. 2 and Fig. 3 for the Beverton-Holt and Ricker birth functions, respectively. By checking the profile of the adult population densities in the n-th year (Fig. 2(d) and Fig. 3(d)), the peaking population density (the maximum value of $u_n(t, x)$ attained in the specific year n for $t \in [0, 1]$ and $x \in [-50, 50]$) will eventually stabilize at a constant level, which is negatively related to the maturation delay. This can be explained as a decreased survival probability $\exp(-d_I\tau)$ with a larger maturation delay. Moreover, the peaking time (the corresponding time instant when $u_n(t, x)$ attains its maximum in year n) occurs at the moment of maturation emergence. Considering the symmetries of the solution profile in the spatial domain, it is interesting to observe that there are two peaking value points for the nonmonotone Ricker birth rate, while

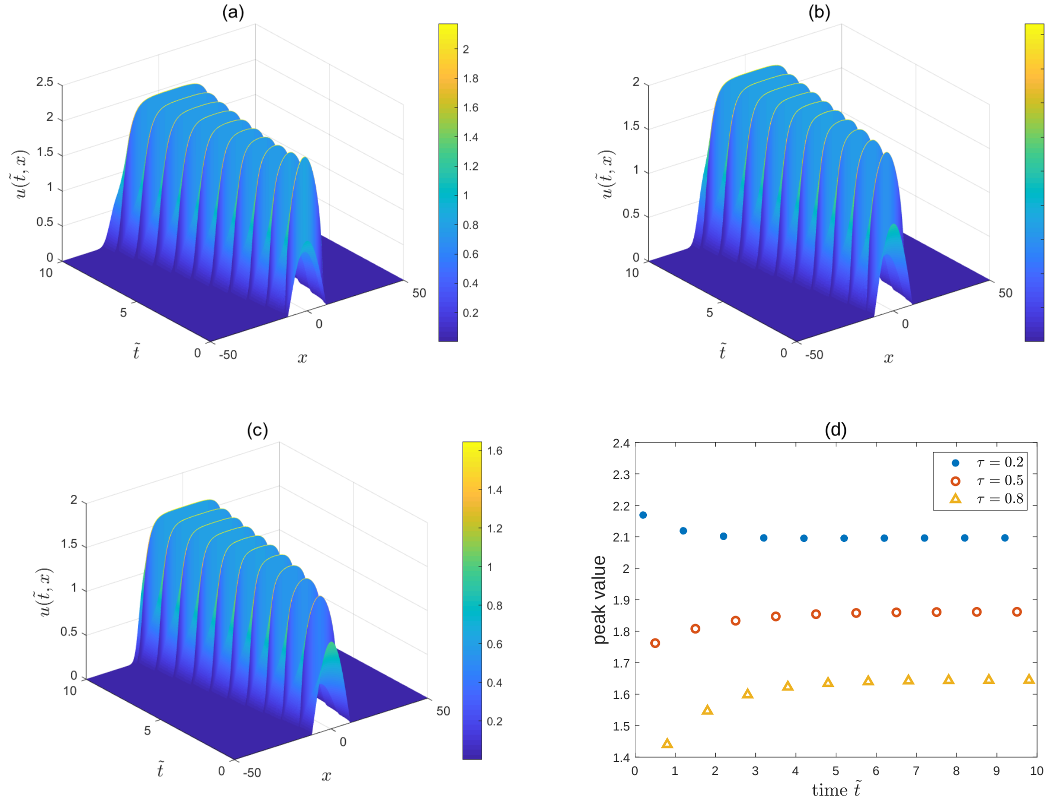

Figure 2: The effects of the maturation emergence time on the population distribution of (2.4) when $g(N)$ is in the Beverton-Holt form. The delay τ for subplots (a), (b) and (c) are 0.2, 0.5 and 0.8, respectively, and $u(\tilde{t},x) := u_n(t,x)$ with $\tilde{t} = n + t$ and $n = \lfloor \tilde{t} \rfloor$. The peaking time and peaking value of the adult population density $u_n(t,x)$ in the n-th year are indicated in subplot (d).

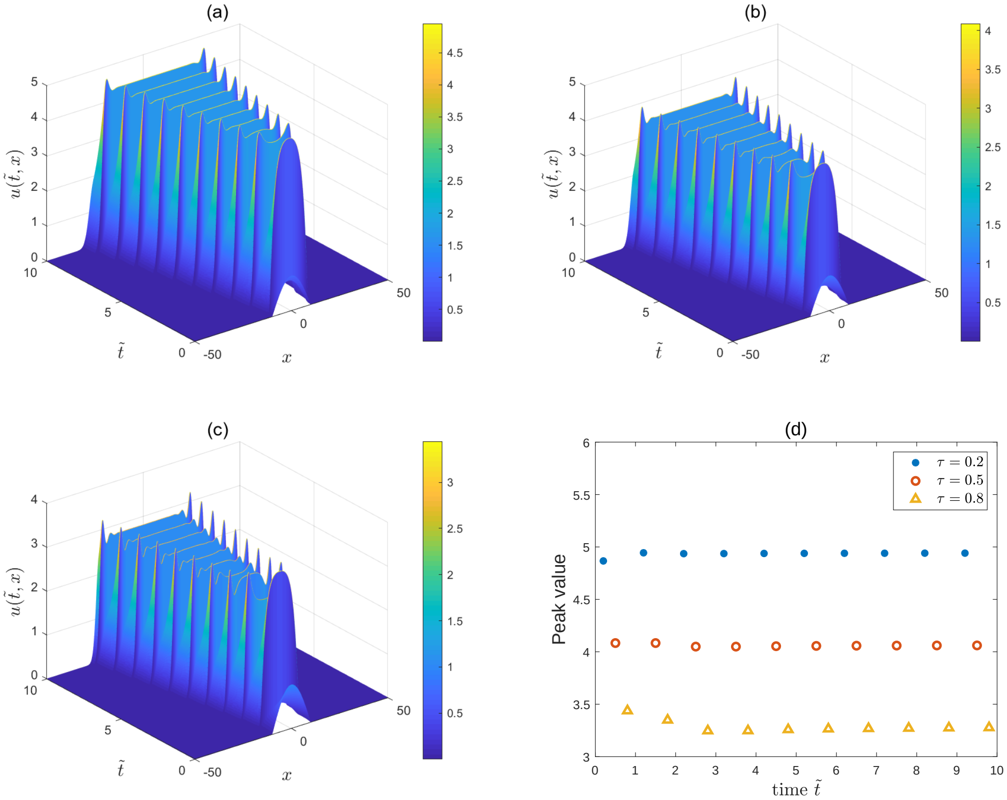

Figure 3: The effects of the maturation emergence time on the population distribution of (2.4) when $g(N)$ takes the Ricker function form. The delay τ for subplots (a), (b) and (c) are $0.2, 0.5$ is 0.8, respectively, and $u(\tilde{t},x) := u_n(t,x)$ with $\tilde{t} = n + t$ and $n = \lfloor \tilde{t} \rfloor$. The peaking time and peaking value of the adult population density $u_n(t,x)$ in the n-th year are indicated in subplot (d).

the peaking value point is unique for the strictly increasing Beverton-Holt birth function. We leave this puzzle for further investigation.

Now we examine the influences of the maturation delay τ on the spreading speed c^*. Noting that when $D_M = D_I$, it follows from Proposition 3.1 that

$$c^* = 2\sqrt{D_M \ln(e^{f'(0)} + g'(0)e^{f'(0)(1-\tau)-d_I\tau})}.$$

This indicates that the monotonicity of c^* with respect to τ is dependent on the sign of $-f'(0)-d_I$. When $D_M < D_I$ and $-f'(0)-d_I > 0$, the whole term of $\Phi(\mu)$ in the Proposition 3.1 is an increasing function of τ and therefore, c^* can be predicted as an increasing function of τ, as shown in Figs. 4(b) and 5(b). This can also be explained by the fact that larger maturation emergence delay increases the distance that the species moves since juveniles with larger diffusion rate takes more time to disperse. When the diffusion rate of adults is greater than that of immatures ($D_M > D_I$), it is surprisingly interesting to find that the monotonicity relationship between the spreading speed c^* and τ can be very complicated, which can be increasing, decreasing, or neither of them (Figs. 4(a) and 5(a)).

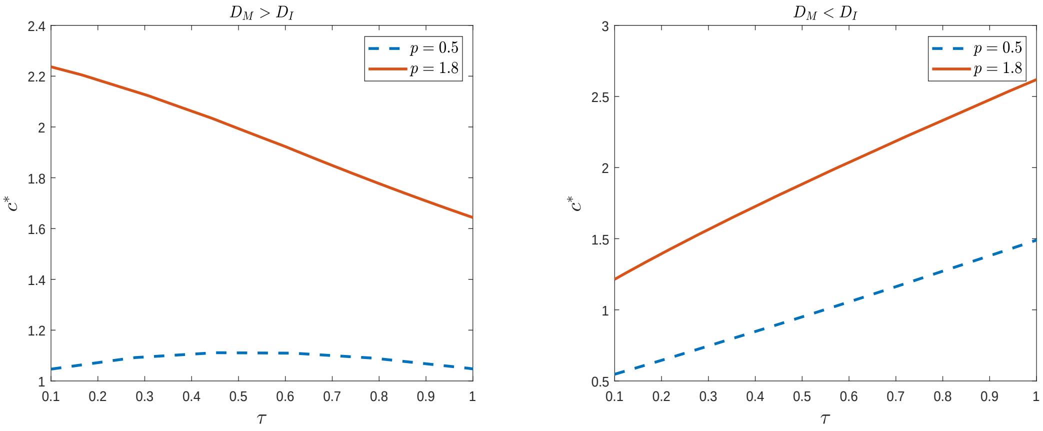

Figure 4: The effects of the maturation delay τ on the spreading speed c^* for different diffusion rates and intrinsic birth rate when $g(N) = \frac{pN}{q+N}$. Left panel: $D_M = 1$, $D_I = 0.2$; right panel: $D_M = 0.2$, $D_I = 1$.

5.2 The effect of the emergence delay on traveling waves

To illustrate the patterns of traveling waves, the matured population densities $N_n(x)$ at different years $n = 9$, 12, 15 through the initial condition

$$N_0(x) = \begin{cases} 5, & x \leqslant -12.5, \\ \frac{1}{5}(12.5 - x), & |x| \leqslant 12.5, \\ 0, & x \geqslant 12.5, \end{cases}$$

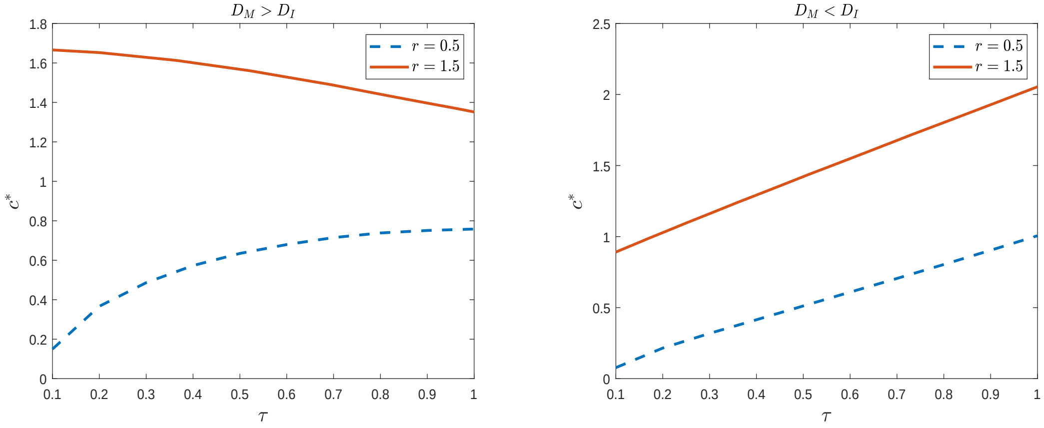

Figure 5: The effects of the maturation delay τ on the spreading speed c^* for different diffusion rates and intrinsic growth rate when $g(N) = Ne^{r-kN}$. Left panel: $D_M = 1$, $D_I = 0.2$; right panel: $D_M = 0.2$, $D_I = 1$.

with different τ values are simulated in Fig. 6. The solutions with the above initial data evolve into a traveling wave solution, with different patterns for the Beverton-Holt function and the Riker function. The wave profiles in Fig. 6(a) for the Beverton-Holt function are monotone, while those in Fig. 6(b) for the Riker birth function are not.

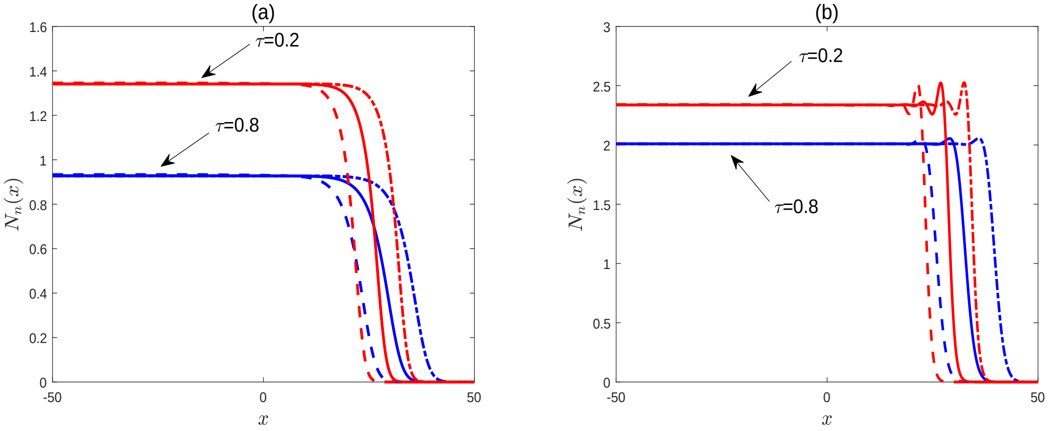

Figure 6: The traveling wave solutions of (2.4) with different birth rate functions: the Beverton-Holt function (left panel) and the Ricker function (right panel). In (a) and (b), dashed lines, solid lines and dash-dotted lines represent $n = 9$, 12, 15, respectively.

5.3 Critical domain size and persistence

In the case where g takes Beverton-Holt function, which is monotone, Fig. 7(a) illustrates the dependence of L^* on D_M with $\tau = 0.5$ and $D_I = \frac{D_M}{5}$. The critical domain size is $L^* = 2.001$ when $D_M = 1$ (see Fig. 7(a)), and $h_\infty = 4.6192$. We see from Fig. 7(b) that the population keeps persistent and approaches to a positive steady state of (4.2) when $L = 3 > L^*$, which is consistent with Theorem 4.1(ii).

In the case where g takes the Ricker function, which is nonmonotone, Fig. 8(a) shows that L^* is a decreasing function of r, when $\tau = 0.5$. When $r = 2.5$, $L^* = 1.8294$ and $h_\infty = 6.1225$. The numerical solution of (4.2) for a domain with length $L = 3$ being greater than $L^* = 1.8294$ is presented in Fig. 8(b).

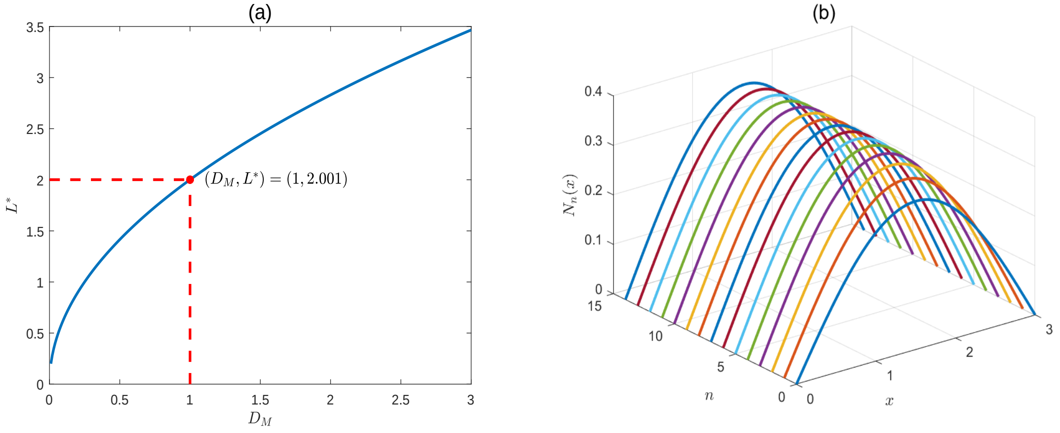

Figure 7: A numerical approximation to the graph of $N_n(x)$ for (4.2) with g taking the Beverton-Holt function.

5.4 Limitations and future research

At the end, we would like to propose further interesting problems related to the current study. The model developed in this manuscript can be extended in several directions, by relaxing some biological assumptions in the model formulation, for example: (i) the model was formulated by assuming that individuals in both immature and matured stages perform random diffusion, which introduces the Laplacian operator in the diffusion term. As a matter of fact, random movement of the species is regarded as a local behavior, which may not be suitable for studying long range interaction of species in a spatial habitat [13]. This motivates one to consider a species with maturation pulse and a nonlocal dispersal represented by an integral (convolution) operator:

$$[\mathcal{A}u](x) = (J * u - u)(x) = \int_{\mathbb{R}} J(x, y)u(y)dy - u(x),$$

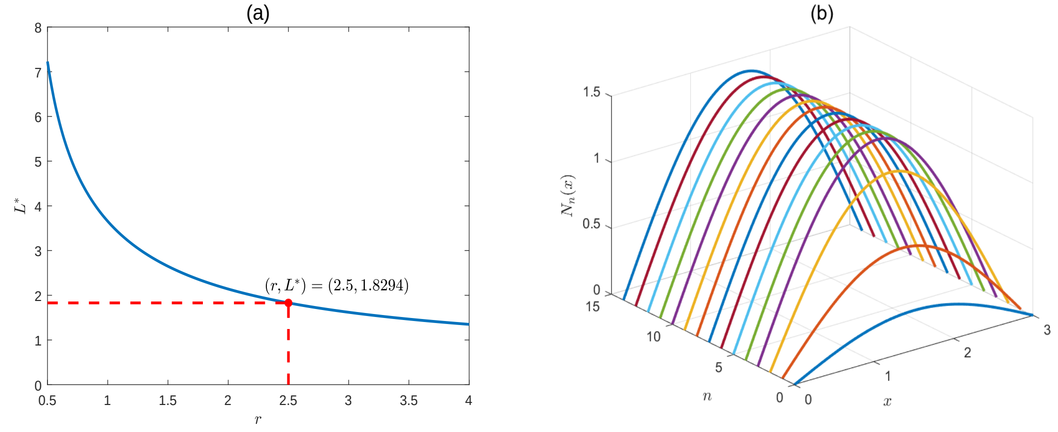

Figure 8: A numerical approximation to the graph of $N_n(x)$ for (4.2) with g taking the Ricker function.

where the dispersal kernel $J(x, y)$ measures the probability distribution for the individuals jumping from location y to location x, which depicts the free and large-range interaction process for species [4, 15]; (ii) another key assumption on model formulation is ignoring the intra-specific competition of immatures. This assumption makes sense for some species as juvenile individuals have the ability to disperse, which can largely alleviates the competition pressure between immature individuals. However, immature individuals of some species with inefficient dispersal ability are subject to strong intra-specific competition for food and resources, which introduces additional density-dependent immature death rate. In this case, the equations for immature and adult population densities can not be decoupled [1, 5, 35]. Further careful derivation of the model and more challenging analysis are needed; (iii) another underlying model assumption is that the new-borns are laid at a rate only dependent on the adult population density, while independent of the spatial location. This is not the case sometimes, for example, when adults may select oviposition habitats [8] or when the habitat ranges for immatures and adults are not exactly the same. In these cases, the impulsive emergence of matured species density $\mathcal{R}(x; N_n)$ in (2.1) should be carefully reformulated. The biological significance and mathematical techniques on addressing these problems are worthy of further investigation.

Acknowledgments

The authors are grateful to two anonymous referees for their valuable comments which led to improvements of our original manuscript.

References

[1] R. Altwegg, Trait-mediated indirect effects and complex life-cycles in two European frogs, *Evol. Ecol. Res.*, 4(2002), 519–536.

[2] Z. Bai, Y. Lou and X.-Q. Zhao, A delayed succession model with diffusion for the impact of diapause on population growth, *SIAM J. Appl. Math.*, 80(2020), 1493-1519.

[3] R. Borowsky and J. Diffley, Synchronized maturation and breeding in natural populations of *Xiphophorus variatus* (Poeciliidae), *Environ. Biol. Fish.*, 6(1981), 49-58.

[4] J. Coville and L. Dupaigne, On a nonlocal equation arising in population dynamics, *Proc. R. Soc. Edinb. Sect. A*, 137(2007), 727-755.

[5] J. Fang, S. Gourley and Y. Lou, Stage-structured models of intra-and inter-specific competition within age classes, *J. Differ. Equ.*, 260(2016), 1918-1953.

[6] M. Fazly, M. Lewis and H. Wang, On impulsive reaction-diffusion models in higher dimensions, *SIAM J. Appl. Math.*, 77(2017), 224-246.

[7] M. Fazly, M. Lewis and H. Wang, Analysis of propagation for impulsive reaction-diffusion models, *SIAM J. Appl. Math.*, 80(2020), 521-542.

[8] S. Gourley and S. Ruan, A delay equation model for oviposition habitat selection by mosquitoes, *J. Math. Biol.*, 65(2012), 1125-1148.

[9] F.C. Hoppensteadt and J.B. Keller, Synchronization of periodical cicada emergences, *Science*, 194(1976), 335-337.

[10] S.-B. Hsu and X.-Q. Zhao, Spreading speeds and traveling waves for nonmonotone integrodifference equations, *SIAM J. Math. Anal.*, 40(2008), 776-789.

[11] W. Jin, H.L. Smith and H.R. Thieme, Persistence and critical domain size for diffusing populations with two sexes and short reproductive season, *J. Dyn. Diff. Equat.*, 28(2016), 689-705.

[12] W. Jin and H.R. Thieme, Persistence and extinction of diffusing populations with two sexes and short reproductive season, *Dis. Cont. Dyn. Sys.*, 19(2014), 3209-3218.

[13] C.-Y. Kao, Y. Lou and W. Shen, Random dispersal vs. nonlocal dispersal, *Dis. Cont. Dyn. Sys.*, 26(2010), 551-596.

[14] M.A. Lewis and B. Li, Spreading speed, traveling wave, and minimal domain size in impulsive reaction-diffusion models, *Bull. Math. Biol.*, 74(2012), 2383-2402.

[15] W.T. Li, J.B. Wang and X.-Q. Zhao, Spatial dynamics of a nonlocal dispersal population model in a shifting environment, *J. Nonlinear Sci.*, 28(2018), 1189-1219.

[16] J. Liang, Q. Yan, C. Xiang and S. Tang, A reaction-diffusion population growth equation with multiple pulse perturbations, *Commun. Nonlinear Sci. Numer. Simul.*, 74(2019), 122-137.

[17] X. Liang, Y. Yi and X.-Q. Zhao, Spreading speeds and traveling waves for periodic evolution systems, *J. Diff. Equ.*, 231(2006), 57-77.

[18] X. Liang and X.-Q. Zhao, Asymptotic speeds of spread and traveling waves for monotone semiflows with applications, *Commun. Pure Appl. Math.*, 60(2007), 1-40.

[19] Y. Lin and Q.-R. Wang, Spreading speed and traveling wave solutions in impulsive reaction-diffusion models, *Commun. Nonlinear Sci. Numer. Simul.*, 23(2015), 185-191.

[20] J. Lu and Z. Guan, *Numerical Solutions of Partial Differential Equations*, second edition, Tsinghua University Press, Beijing, 2004.

[21] M.B. Mohring, T. Wernberg, G.A. Kendrick, et al., Reproductive synchrony in a habitat-forming kelp and its relationship with environmental conditions, *Mar. Biol.*, 160(2013), 119-126.

[22] R. Peng and X.-Q. Zhao, The diffusive logistic model with a free boundary and seasonal succession, *Dis. Cont. Dyn. Sys.*, 33(2013), 2007-2031.

[23] C. Riehl, Reproductive Synchrony, In: J. Vonk and T. Shackelford (eds) *Encyclopedia of Animal Cognition and Behavior*, Springer, Cham, 2018.

[24] R.G. Santos, H.T. Pinheiro, A.S. Martins, et al., The anti-predator role of within-nest emergence synchrony in sea turtle hatchlings, *Proc. R. Soc. B: Biol. Sci.*, 283(2016), 20160697.

[25] T. Shlesinger and Y. Loya, Breakdown in spawning synchrony: A silent threat to coral persistence, *Science*, 365(2019), 1002-1007.

[26] H.L. Smith, *Monotone Dynamical Systems: An Introduction to the Theory of Competitive and Cooperative Systems*, Math. Surveys Monographs, 41, Amer. Math. Soc., Providence, RI, 1995.

[27] C.M. Taylor and A. Hastings, Allee effects in biological invasions, *Ecol. Lett.*, 8(2005), 895-908.

[28] A. Veprauskas, Synchrony and the dynamic dichotomy in a class of matrix population models, *SIAM J. Appl. Math.*, 78(2018), 2491-2510.

[29] A. Veprauskas and J.M. Cushing, A juvenile-adult population model: climate change, cannibalism, reproductive synchrony, and strong Allee effects, *J. Biol. Dyn.*, 11(2017), 1-24.

[30] Z. Wang and H. Wang, Persistence and propagation of a PDE and discrete-time map hybrid animal movement model with habitat shift driven by climate change, *SIAM J. Appl. Math.*, 80(2020), 2608-2630.

[31] K.S. Williams, K.G. Smith and F.M. Stephen, Emergence of 13-Yr periodical cicadas (*Cicadidae: Magicicada*): phenology, mortality, and predators satiation, *Ecology*, 74(1993), 1143-1152.

[32] R. Wu and X.-Q. Zhao, Spatial invasion of a birth pulse population with nonlocal dispersal, *SIAM J. Appl. Math.*, 79(2019), 1075-1097.

[33] R. Wu and X.-Q. Zhao, The evolution dynamics of an impulsive hybrid population model with spatial heterogeneity, *Commun. Nonlinear Sci. Numer. Simul.*, 107(2022), 106181.

[34] X. Yu and X.-Q. Zhao, A periodic reaction-advection-diffusion model for a stream population, *J. Diff. Equ.*, 258(2015), 3037-3062.

[35] L. Zhang, K. Liu, Y. Lou and Z.-C. Wang, Spatial dynamics of a nonlocal model with periodic delay and competition, *Eur. J. Appl. Math.*, 31(2020), 1070-1100.

[36] X.-Q. Zhao, *Dynamical Systems in Population Biology*, second edition, Springer, New York, 2017.